

Probing hadronization and freeze-out with multiple strange hadrons and strange resonances

Marcus Bleicher^a

^aSUBATECH, Laboratoire de Physique Subatomique et des Technologies Associées,
University of Nantes - IN2P3/CNRS - Ecole des Mines de Nantes,
4 rue Alfred Kastler, F-44072 Nantes Cedex 03, France

The major goal of the various heavy ion programs is the search for a transient state of deconfined matter, dubbed the quark-gluon-plasma (QGP): A phase transition to this new state of matter is predicted by lattice QCD when a sufficiently high energy density ($\epsilon \approx 1 \text{ GeV/fm}^3$) is reached.

Strange particle yields and spectra are key probes to study excited nuclear matter and to detect the transition of (confined) hadronic matter to quark-gluon-matter (QGP) [1, 2]. The relative enhancement of strange and multi-strange hadrons, as well as hadron ratios in central heavy ion collisions with respect to peripheral or proton induced interactions have been suggested as a signature for the transient existence of a QGP-phase [2].

A wealth of systematic information has been gathered to study the energy dependence of observables from $\sqrt{s} \approx 2 \text{ AGeV}$ to $\sqrt{s} = 200 \text{ AGeV}$. For the first time also information on unstable particle emission in AA reactions is available: the Φ and $\Lambda(1520)$ have been observed in heavy ion reactions at SPS energies [3], SPS and RHIC experiments [3, 4] report measurements of the $\bar{K}^0(892)$ signal, and RHIC is already attacking the f_0 and ρ mesons and the $\Sigma(1385)$.

A key problem is the identification of unambiguous signatures of possible QGP creation. Under the assumption of thermal and chemical equilibrium, fits with a statistical (thermal) model have been used to extract bulk properties of hot and dense matter, e.g. the temperature and chemical potential at which chemical freeze-out occurs [5, 6, 7]. In addition also dynamical evaporation models and non-equilibrium transport calculations have been employed to study the energy and centrality dependence of particle and especially strangeness production [8, 9, 10, 11]. Overall, the conclusions are ambiguous and range from evidence for QGP creation to canonical enhancement and from string fusion to baryon junctions.

Numerous ideas have been brought forward in the past, ranging from the search for a softest point in the equation of state, photon and lepton radiation, J/Ψ suppression to event-by-event fluctuations. However, the main difficulty in the interpretation of the available data is that the observed final state hadrons carry relatively little information about their primordial sources. Most of the hadrons had been subject to many secondary interactions and are strongly influenced by the decays of high mass resonances. To shed some light on the strangeness production mechanism and the question of chemical and

kinetic equilibration and decoupling, we study

- the production of multiple strange baryons in pp interactions. Here on can directly probe the microscopic decay of color flux tubes, allowing to differentiate between different string models and a statistical description of the hadronization.
- The energy and centrality dependence of (strange) hadron resonances in AA which carry unique information about the stage between chemical and kinetic freeze-out.

Hadronization in proton-proton interactions

In the string picture, high energy proton-proton collisions create “excitations” in form of strings, being one dimensional objects which decay into hadrons according to longitudinal phase space. This framework is well confirmed in low energy electron-positron annihilation [12] where the virtual photon decays into a quark-anti-quark string which breaks up into various kinds of hadrons. However, specific string models differ in their philosophy and the types of strings that are created. In general two classes of models - based on color or momentum exchange - can be distinguished, the resulting objects two quark-diquark strings with valence quarks being their ends, however, is quite similar. Here we will contrast the present UrQMD prescription for string formation (similar to the PYTHIA model [13] with the approach used in NeXuS 3.0: In UrQMD[14] the projectile and target protons become excited objects due to the momentum transfer in the interaction. The resulting strings, with at most two strings being formed, are of the di-quark-quark type.

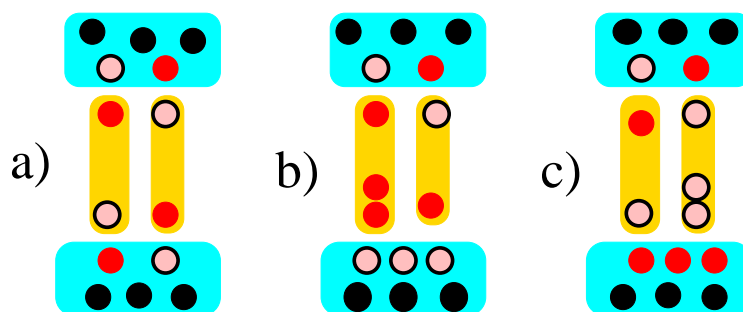


Figure 1. a) The simplest collision configuration has two remnants and one cut Pomeron represented by two $q-\bar{q}$ strings. b) One of the \bar{q} string-ends can be replaced by a qq string-end. c) With the same probability, one of the q string-ends can be replaced by a $\bar{q}\bar{q}$ string-end (taken from [18]).

In NeXuS 3.0[15], the pp interaction is described in terms of Pomeron exchanges or ladder diagrams. Both hard and soft interactions take place in parallel. Energy is shared equally between all cut Pomerons and the remnants. Here, for the string ends of soft and semi-hard Pomerons quarks and anti-quarks from the sea are taken in a flavour-symmetric way. Thus, the valence quarks stay in the remnants, yielding excited quark bags [18] (see

Fig. 1). In contrast to these string models, the predictions of two statistical models (model **I**, being fully canonical [16] and model **II**, being canonical with respect to strangeness [17]) are also shown.

Fig. 2 (left) depicts the anti-baryon to baryon ratio at midrapidity in proton proton interactions at 160 GeV. The results of the calculations by the new NeXuS 3.0 (ratios calculated from [18]) and UrQMD/PYTHIA, which are well established string-fragmentation models for elementary hadron hadron interactions, are included in this figure. In both di-quark models, the \bar{B}/B ratio increases strongly with the strangeness content of the baryon. For strangeness $|s| = 3$ the ratio significantly exceeds unity. In UrQMD and PYTHIA the hadronization of the di-quark-quark strings leads directly to the overpopulation of $\bar{\Omega}$ as discussed in detail in [19]. The new string formation scheme employed in NeXuS 3.0, however, allows to get a reasonable agreement with experimental data. The basic features of the production of multi-strange baryons as well as of Λ s and protons can be understood within the model picture of proton-proton scattering: the created final particles emerge from a non-trivial system of projectile/target remnant states and a number of cut Pomerons each represented by a pair of strings.

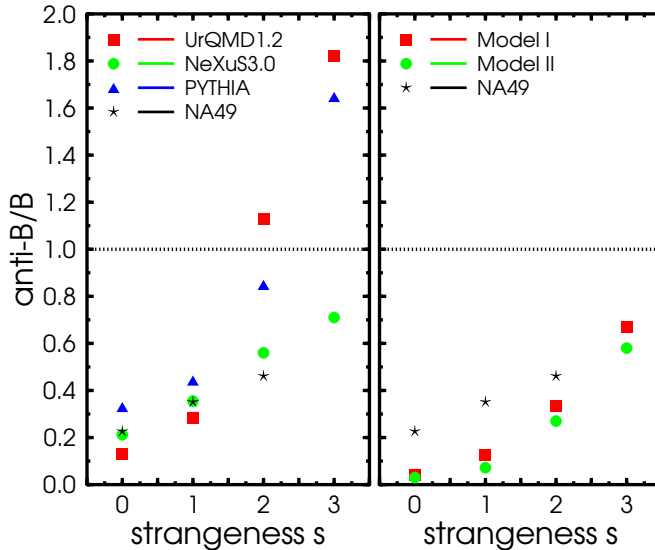


Figure 2. Left: anti-baryon to baryon ratio at $|y - y_{\text{cm}}| < 1$ in pp interactions at 160 GeV as given by PYTHIA, NeXuS3.0 and UrQMD. Right: anti baryon to baryon ratio for the same reaction as given by statistical models. Stars depict preliminary NA49 data for the \bar{B}/B ratio at midrapidity.

The predictions of the statistical models (in full phase space) are shown in Fig. 2 (right). In these approaches the \bar{B}/B ratio is seen to exhibit a significantly weaker increase with the strangeness content of the baryon than expected in the di-quark string fragmentation models. In the grand canonical picture, where the \bar{B}/B ratio is very sensitive to the baryon chemical potential μ_B , it is easily understood that statistical models, can not yield a ratio of $\bar{\Omega}/\Omega > 1$. For finite baryon densities as in the pp system, the \bar{B}/B has to stay below one and only in the limit of $\mu_B = 0$ may $\bar{\Omega}/\Omega = 1$ be approached. This

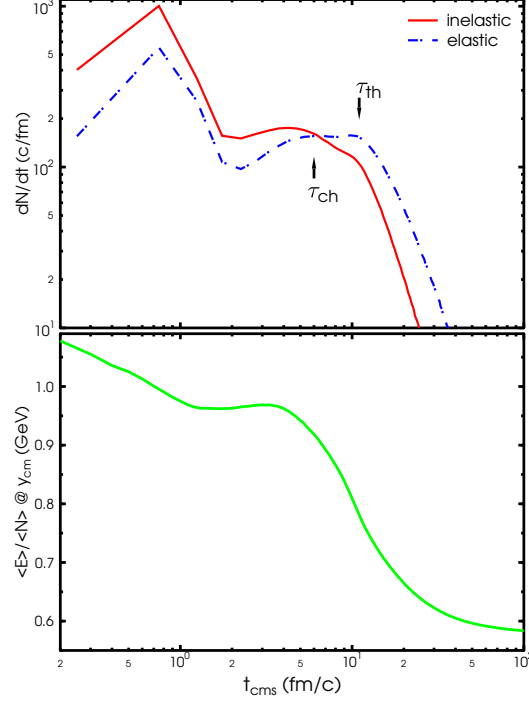


Figure 3. Top: Inelastic and (pseudo-)elastic collision rates in Pb+Pb at 160A GeV. τ_{ch} and τ_{th} denote the chemical and thermal/kinetic freeze-out as given by the microscopic reaction dynamics of UrQMD. Bottom: Average energy per particle at midrapidity ($|y - y_{\text{cm}}| \leq 0.1$) as a function of time (taken from [23]).

feature is not blurred in the canonical approach. For comparison, both figures include preliminary data on the \bar{B}/B ratios obtained at midrapidity by the NA49 Collaboration [20] (Very preliminary NA49 data seems to support a $\bar{\Omega}/\Omega$ ratio below one [21]).

It is important to note that the result $\bar{\Omega}/\Omega > 1$ in pp collisions from the di-quark string models solely depends on the geometry of the decaying objects. The ratio can not be altered (or even inverted) by modifications of the strangeness and di-quark suppression factors. These factors can only modify the absolute yields of strange hadrons, but do not influence the ratio discussed here.

If the new NA49 data can be confirmed, one is forced to conclude that the di-quark string models fail to describe the ratios of multiple strange baryons in pp interactions at the SPS. A solution might be to replace the conventional approach by a system of sea quark strings and remnants or to abandon the flux tube picture, which has explained many dynamical features of hh collisions, for a statistical hadronization model.

Chemical and kinetic freeze-out in AA collisions

In nucleus-nucleus collisions the situation is by far more involved than in the pp case discussed above. Here, the major fraction of finally observed particles in the experimental setup stem from decays of resonances (mesonic or baryonic) which have undergone many scatterings from their point of production to observation. The final hadron yields seem to be compatible with a hadronic gas described by the baryo-chemical potential μ_B and

a temperature parameter T in a statistical model (see e.g. [5, 6, 7]). It has been suggested that both parameters are coupled by a universal freeze-out criterion assuming a mean energy per hadron $\langle E \rangle / \langle N \rangle = 1$ GeV/hadron [22] at chemical freeze-out. In this framework, the formed hadrons do only undergo elastic collision from this chemical freeze-out time (at SPS energies at a temperature of $\approx 160 - 170$ MeV to the final kinetic freeze-out at temperatures of the order of 120 MeV).

To explore whether this sequential freeze-out is realized in heavy ion reactions at highest energies and how it can be probed, the Ultra-relativistic Quantum Molecular Dynamics model (UrQMD 1.2) is used [14]. This microscopic transport approach is based on the covariant propagation of constituent quarks and di-quarks accompanied by mesonic and baryonic degrees of freedom. As discussed above, the leading hadrons of the fragmenting strings contain the valence-quarks of the original excited hadron and represent a simplified picture of the leading (di)quarks of the fragmenting string. The elementary hadronic interactions are modelled according to measured cross sections and angular distributions. If the cross sections are not experimentally known, detailed balance is employed in the energy range of resonances. The partial and total decay widths are taken from the Particle Data Group.

To analyse the different stages of a heavy ion collision, Fig. 3 (top) depicts the time evolution of the elastic and inelastic collision rates in central Pb+Pb interactions at 160A GeV. The inelastic collision rate (full line) is defined as the number of collisions with flavour changing processes (e.g. $\pi\pi \rightarrow K\bar{K}$). The elastic collision rate (dashed dotted line) consists of two components, true elastic processes (e.g. $K\pi \rightarrow K\pi$) and pseudo-elastic processes (e.g. $K\pi \rightarrow K^* \rightarrow K\pi$). While elastic collision do not change flavour, pseudo-elastic collisions are different. Here, the ingoing hadrons are destroyed and a resonance is formed. If this resonance decays later into the same flavours as its parent hadrons, this scattering is pseudo-elastic. Fig. 3 (bottom) depicts the average thermal energy - calculated from interacted hadrons with $p_z^2 = (p_x^2 + p_y^2) / 2$ - per particle at midrapidity ($|y - y_{\text{cm}}| \leq 0.1$).

The present microscopic study of the collision dynamics, indeed supports the idea of separated phases in the evolution of the system:

- I** $t < 2$ fm/c: In the initial stage of the nucleus-nucleus reaction non-equilibrium dynamics leads to strong baryon stopping in multiple inelastic interactions, shown by huge and strongly time dependent collision rates. This stage deposits a large amount of (non-thermalized) energy and creates the first generation particles.
- II** $2 \text{ fm/c} < t < 6 \text{ fm/c}$: Due to the high particle densities and energies inelastic scatterings dominate this stage of the reaction. Chemical equilibrium might be achieved due to a large number of flavour and hadro-chemistry changing processes until chemical freeze-out.
- III** $6 \text{ fm/c} < t < 11 \text{ fm/c}$: After the system has expanded and cooled down, elastic and pseudo-elastic collisions take over. Here, only the momenta of the hadrons change, but the chemistry of the system is mainly unaltered, leading to the kinetic freeze-out of the system.

IV $t > 11$ fm/c: Finally, the reactions cease and the scattering rates drop drastically. The systems breaks up.

Even the hypothesis of chemical decoupling at an energy per hadron of 1 GeV, is in line with our analysis as demonstrated in Fig. 3 (bottom). In the non-equilibrium stage $\langle E \rangle / \langle N \rangle$ decreases steadily. While the system is 'cooking' in the inelastic scattering stage, $\langle E \rangle / \langle N \rangle$ stays constant around 1 GeV and drops suddenly as the hadronic system enters the kinetic stage.

The spectra and abundances of $\Lambda(1520)$, $K^0(892)$ and other resonances can be used to study the break-up dynamics of the source between chemical and thermal freeze-out. If chemical and thermal freeze-out are not separated - e.g. due to an explosive break-up of the source - all initially produced resonances are reconstructable by invariant mass analysis of the final state hadrons. However, if there is a separation between the different freeze-outs, a part of the resonance daughters rescatter, making this resonance unobservable in the final state. Thus, the relative suppression of resonances in the final state compared to those expected from thermal estimates provides a chronometer for the time period between the different reaction stages. Even the chemical composition of the system might be changed by up to 10% in the hyperon sector (after chemical 'freeze-out'), due to inelastic scatterings of the resonance daughters (e.g. $\bar{K}p \rightarrow \Lambda$).

The rapidity spectra for $\Delta(1232)$, $\Lambda^*(1520)$, $K^0(892)$ and Φ in Pb(160 AGeV)Pb, $b < 3.4$ fm collisions. are depicted in Fig. 4. The left part, shows the total amount of decaying

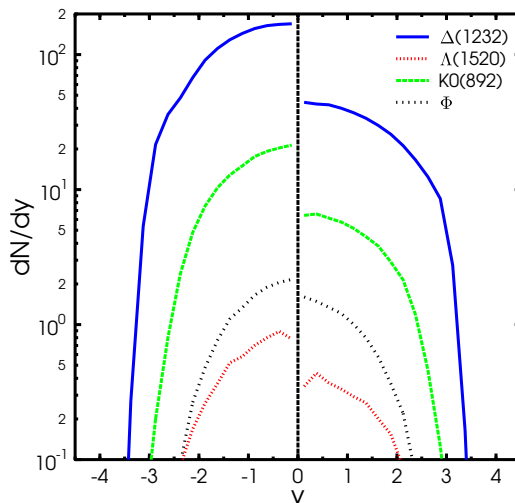


Figure 4. Rapidity densities for $\Delta(1232)$, $\Lambda^*(1520)$, $K^0(892)$ and Φ in Pb(160 AGeV)Pb, $b < 3.4$ fm collisions. Left: All resonances as they decay. Right: Reconstructable resonances (taken from [23]).

resonances. Here, subsequent collisions of the decay products have not been taken into account - i.e. whenever a resonance decays during the systems evolution it is counted. However, the additional interaction of the daughter hadrons disturbs the signal of the

resonance in the invariant mass spectra. This lowers the observable yield of resonances drastically as compared to the primordial yields at chemical freeze-out. Fig. 4 (right) addresses this in the rapidity distribution of those resonances whose decay products do not suffer subsequent collisions - these resonances are in principle reconstructable from their decay products. Note that reconstructable in this context still assumes reconstruction of all decay channels, including many body decays.

By using the estimates done by [24] in a statistical model, it seems possible to relate the result of the present microscopic transport calculation to thermal freeze-out parameters. The surprising result is that the microscopic source seems to have a lifetime shorter than 1 fm/c and a freeze-out temperature lower than 100 MeV. Apparently, the values obtained from UrQMD seem to favour a scenario of a sudden break-up of the initial hadron source, in contrast to the time evolution of the chemical and thermal decoupling as shown in Fig. 3. This misleading interpretation might be due to the re-creation of resonances in the elastic scattering stage, which was not taken into account in the statistical model analysis. The influence of these effects is currently under investigation.

However, even the question of the existence of such resonance states in the hot and dense environment is still not unambiguously answered. Since hyperon resonances are expected to dissolve at high energy densities (see .e.g. [25]) it is of utmost importance to study the cross section of hyperon resonances as a thermometer of the collision.

To set the stage, Figs. 5 and 6 address the excitation function of observable resonance multiplicities. In addition, a comparison of rapidity integrated yields (4π values, circles) with the center-of-mass values ($y_{\text{cm}} \pm 0.5$, squares) is given. The Λ includes decays from Σ^0 , but not from Ξ . Protons do not include decays from Λ 's. All strong decays are included. No cuts are applied except when mentioned. The anti- K^* multiplicities are monotonously increasing with energy, while the hyperon resonance show a pronounced maximum in the excitation function at $\sqrt{s} = 8$ GeV ($E_{\text{lab}} \approx 30$ AGeV). This maximum is also present - as earlier observed for hyperons by [26] - if scaled by the number of pions. This makes the newly planned GSI200 facility an ideal place to study in-medium modifications of resonances.

More information can be obtained if the multiplicities are normalised to the groundstate hadrons, i.e. (anti-)Kaons and Lambdas. Figs. 7 and 8 show the energy dependence of the h^*/h ratios. Here the baryo-chemical potentials cancel out and information on the freeze-out temperature can be obtained.

To summarise, hadronization into multiple strange hadrons in elementary pp interactions has been studied within different string approaches and statistical models and confronted with data. Di-quark string models seem not to be in line with the experimental observations of $\bar{\Omega}$ and Ω production in pp at the SPS. The freeze-out dynamics in AA has been microscopically explored. Different decoupling stages have been identified in the non-equilibrium dynamics. Observables to clock the kinetic scattering stage and the freeze-out temperature with (strange-) resonances were discussed.

Acknowledgements

I want to acknowledge interesting and stimulating discussions with Drs. Klaus Werner, Jörg Aichelin, Fuming Liu, Tanguy Pierog, Christina Markert and Giorgio Torrieri.

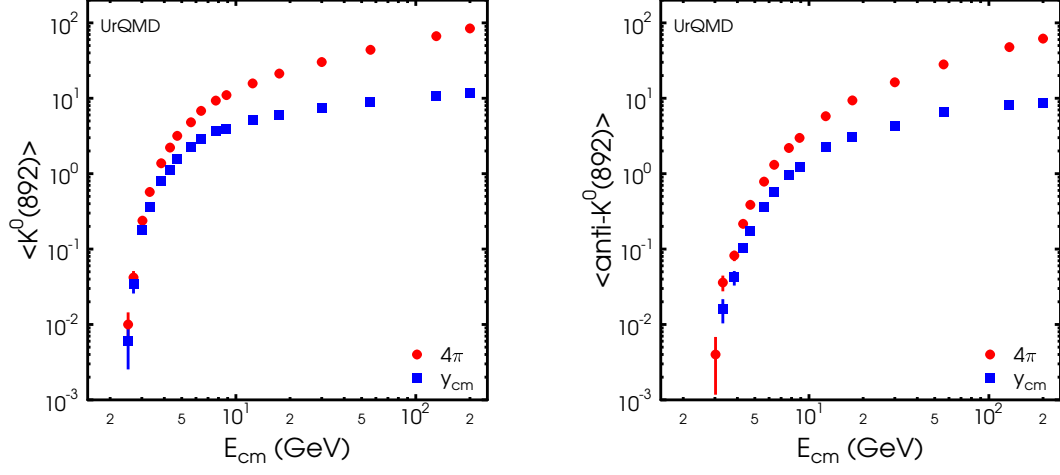


Figure 5. Multiplicity excitation function for central Pb+Pb (Au+Au) reactions, in 4 π (circles) and at midrapidity (squares). Left: $\langle K^0(892) \rangle$. Right: $\langle \overline{K}^0(892) \rangle$.

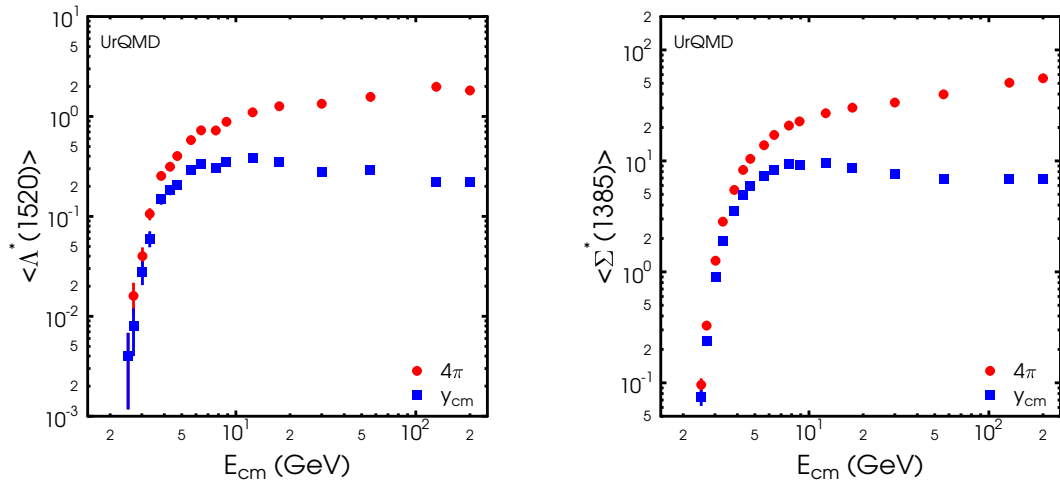


Figure 6. Multiplicity excitation function for central Pb+Pb (Au+Au) reactions, in 4 π (circles) and at midrapidity (squares). Left: $\langle \Lambda^*(1520) \rangle$. Right: $\langle \Sigma^*(1385) \rangle$ (all charges summed).

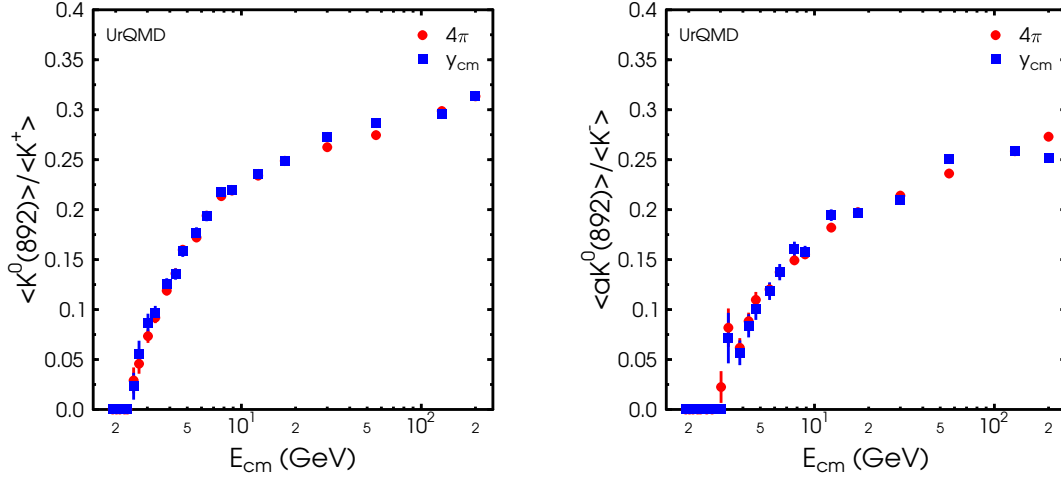


Figure 7. Ratio excitation function for central Pb+Pb (Au+Au) reactions, in 4π (circles) and at midrapidity (squares). Left: $\langle K^0(892) \rangle / \langle K^+ \rangle$. Right: $\langle \bar{K}^0(892) \rangle / \langle K^- \rangle$.

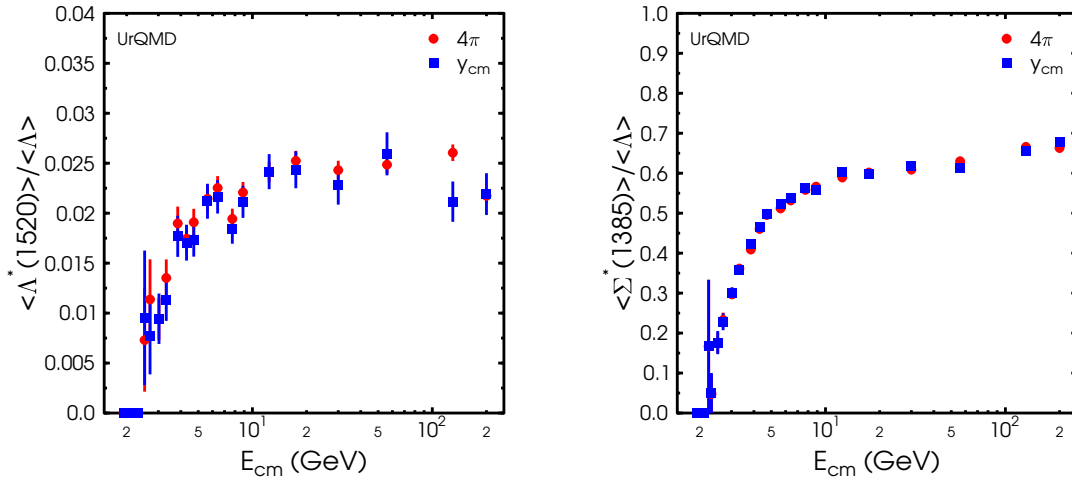


Figure 8. Ratio excitation function for central Pb+Pb (Au+Au) reactions, in 4π (circles) and at midrapidity (squares). Left: $\langle \Lambda^*(1520) \rangle / \langle \Lambda \rangle$. Right: $\langle \Sigma^*(1385) \rangle / \langle \Lambda \rangle$.

REFERENCES

1. S. A. Bass, M. Gyulassy, H. Stöcker and W. Greiner, J. Phys. **G25**, R1 (1999); Stock R, Phys. Lett. **B456**, (1999) 277
2. J. Rafelski and B. Müller, Phys. Rev. Lett. **48**, 1066 (1982); J. Rafelski, Phys. Rep. **88**, 331 (1982); P. Koch, B. Müller and J. Rafelski, Phys. Rep. **142**, 167 (1986).
3. Ch. Markert, PhD thesis, Univ. Frankfurt; V. Fries [NA49 collaboration], <http://www.rhic.bnl.gov/qm2001/>
4. Z. b. Xu [STAR Collaboration], Nucl. Phys. A **698** (2002) 607 [arXiv:nucl-ex/0104001]. For the latest results, see these proceedings.
5. J. Letessier, A. Tounsi, U. Heinz, J. Sollfrank and J. Rafelski, Phys. Rev. Lett. **70**, 3530 (1993); J. Letessier, J. Rafelski and A. Tounsi, Phys. Lett. **B321**, 394 (1994); J. Rafelski and M. Danos, Phys. Rev. **C50**, 1684 (1994).
6. J. Cleymans and K. Redlich, Phys. Rev. Lett. **81**, 5284 (1998); F. Becattini, J. Cleymans, A. Keranen, E. Suhonen and K. Redlich, Phys. Rev. **C64**, 024901 (2001).
7. P. Braun-Munzinger, J. Stachel, J. P. Wessels and N. Xu, Phys. Lett. **B344**, 43 (1995); **B365**, 1 (1996); P. Braun-Munzinger, I. Heppe and J. Stachel, Phys. Lett. **B465**, 15 (1999); P. Braun-Munzinger, D. Magestro, K. Redlich and J. Stachel, Phys. Lett. **B518**, 41 (2001).
8. C. Spieles, H. Stocker and C. Greiner, Eur. Phys. J. **C2** 351 (1998) 351; C. Greiner and H. Stöcker., Phys. Rev. **D44**, 3517 (1992).
9. S. A. Bass et al., Phys. Rev. Lett. **81**, 4092 (1998).
10. S. Soff, S. A. Bass, M. Bleicher, L. Bravina, E. Zabrodin, H. Stocker and W. Greiner, Phys. Lett. B **471** (1999) 89 [arXiv:nucl-th/9907026].
11. S. E. Vance and M. Gyulassy, Phys. Rev. Lett. **83** (1999) 1735
12. K. Werner, Phys. Rept. **232** (1993) 87.
13. H.-U. Bengtsson and T. Sjöstrand, Comput. Phys. Commun. **46** 43 (1987).
14. M. Bleicher et al., J. Phys. **G25** 1859 (1999); S. A. Bass et al., Prog. Part. Nucl. Phys. **41** 225 (1998).
15. H.J. Drescher et al., Phys. Rep. **350** 93 (2001).
16. F. Becattini and G. Passaleva, hep-ph/0110312, Eur. Phys. J. in print.
17. J. S. Hamieh, K. Redlich and A. Tounsi, Phys. Lett. **B486** 61 (2000); J. Phys. **G27**, 413 (2001).
18. F. M. Liu, J. Aichelin, M. Bleicher, H. J. Drescher, S. Ostapchenko, T. Pierog and K. Werner, arXiv:hep-ph/0202008.
19. M. Bleicher et al., Phys. Rev. Lett. **88** (2002) 202501 [arXiv:hep-ph/0111187].
20. T. Susa et al, NA49, Nucl. Phys. A698 (2002) 491c; K. Kadija, talk given at *Strange Quark Matter 2001*, Frankfurt, Germany.
21. NA49 Collaboration, Proposal CERN/SPSC/P264, Addendum 10
22. J. Cleymans and K. Redlich, Phys. Rev. Lett. **81** (1998) 5284 [arXiv:nucl-th/9808030].
23. M. Bleicher and J. Aichelin, Phys. Lett. B **530** (2002) 81 [arXiv:hep-ph/0201123].
24. G. Torrieri and J. Rafelski, Phys. Lett. B **509** (2001) 239 [arXiv:hep-ph/0103149].
25. M. F. Lutz and C. L. Korpa, arXiv:nucl-th/0105067.
26. P. Braun-Munzinger, J. Cleymans, H. Oeschler and K. Redlich, Nucl. Phys. A **697** (2002) 902 [arXiv:hep-ph/0106066].